Data-driven inversion of GPR surface reflection data for lossless layered media

(Invited Paper)

Evert Slob and Kees Wapenaar
Department of Geoscience & Engineering, Delft University of Technology, Delft, Netherlands,
e.c.slob@tudelft.nl, c.p.a.wapenaar@tudelft.nl

***Abstract*—Two wavefields can be retrieved from the measured reflection response at the surface. One is the Green's function at a chosen virtual receiver depth level in a layered model generated by a source at the surface. The other wavefield consists of the upgoing and downgoing parts of a wavefield that focuses at the virtual receiver depth level. From the upgoing part of the focusing wavefield an image can be computed at one-way vertical travel time and with correct amplitudes of the local reflection coefficients as a function of incidence angle. These reflection coefficient values can be used to invert for electric permittivity and magnetic permeability. From these values and the known image times the layer thickness values can be obtained for each layer. This method renders the full waveform inversion problem for horizontally layered media a linear problem.**

***Index Terms*—antenna, propagation, measurement.**

I. Introduction

Normally one solves the inverse problem using a data-misfit criterion, which is an iterative forward modeling approach to inversion. This approach does not directly retrieve information from the data, but uses the data to fit the modeled data to. This is a model driven approach to solving the inverse problem. Retrieving information directly from the measured data will constitute a data-driven approach to solving the inverse problem. It can be called a full waveform data inversion method if the electric and magnetic parameters are obtained as a function of subsurface position. In this paper we investigate a new method to obtain the electric and magnetic medium properties of a horizontally layered medium from the measured data.

From seismic interferometry we know that virtual sources (or receivers) can be created at physical receivers (or sources) [1], [2], [3]. If these are in the subsurface the reflection response of the medium below the receiver (or source) level can be obtained through multidimensional deconvolution of the upgoing wavefield by the downgoing wavefield at this level [4], [5]. To obtain information below this level, model driven methods are being used to first create reflection images and then medium parameters are estimated from the reflection coefficients.

In a new approach, surface reflection data is computed from the measured data. In this step sources are redatumed to the receiver level. The reflection data is used to create a virtual Vertical Radar Profile (VRP) by creating a virtual receiver in the subsurface using physical receivers at the surface. The sources remain at their redatumed positions. Hence, virtual receivers are created in the subsurface without needing physical sources or receivers in the subsurface. This approach retrieves the up- and downgoing wavefields at the virtual receiver depth level separately and finds the true amplitude image directly from the upgoing wavefield. Amplitude versus angle analysis in the tau-p domain will give the medium parameters.

Here we show how the method exploits internal multiples in the reflection response of a layered earth to obtain correct amplitudes of the primary reflections and avoids creating ghosts images from the internal multiple reflections at the same time. This can be done using the recently developed theory [6], which is an acoustic theory inspired by 1D focusing theory [7], but valid in 3D heterogeneous media. The scheme is non-recursive in depth and hence the method does not suffer from error propagation.

The full waveform inversion problem is cast as a three-step linear problem. First an image is obtained by filtering the measured reflection response. Then the image amplitudes as a function of incidence angle are used to compute the electric permittivity and magnetic permeability inside each layer. Finally the medium parameters in each layer are used to convert image times to image depth values and hence layer thickness values are obtained. We show each of these three steps and illustrate the method with a numerical example using the TE-mode reflection response.

II. Obtaining the reflection response from the measured data

We use the vector $\mathbf{x} = (x, y, z)$ to denote the coordinate vector of a point in three-dimensional space, with the vertical axis pointing downward, and we work in the frequency domain assuming $\exp(\mathrm{i}\omega t)$ time dependence, with i the imaginary unit, $\omega = 2\pi f$ radial frequency, f is natural frequency, and t denotes time. For a horizontally layered medium with interfaces at depth levels z_i, $i = 0, 1, 2, \cdots$, the sources are assumed to be located at depth level $z^s < 0$ and the receivers at depth level $z^r < 0$ but such that $z^r > z^s$. It is well-known that in a homogeneous subdomain the electromagnetic field can be decomposed in upgoing and downgoing waves and in TE- and TM-modes [8], [9]. This decomposition is most easily carried out in the horizontal wavenumber domain because then it can be carried out for each wavenumber separately. We apply a two-dimensional spatial Fourier transformation with

$\exp(\mathrm{i}\boldsymbol{k}_T \cdot \mathbf{x}_T)$ as Fourier kernel; $\boldsymbol{k}_T = (k_x, k_y, 0)$ and a similar definition holds for $\mathbf{x}_T$. Quantities in the horizontal Fourier transformed-frequency domain are denoted with a diacritical tilde, e.g., the electric field vector is denoted $\tilde{\boldsymbol{E}}$. Here we use the procedure of [5] and store the measured horizontal components of the electric, $\tilde{\boldsymbol{E}}$, and the magnetic, $\tilde{\boldsymbol{H}}$, field vectors in the field vector $\tilde{\boldsymbol{F}}$ as $\tilde{\boldsymbol{F}} = (\tilde{\boldsymbol{F}}_1, \tilde{\boldsymbol{F}}_2)$, with $\tilde{\boldsymbol{F}}_1 = (\tilde{E}_x, \tilde{E}_y)$ and $\tilde{\boldsymbol{F}}_2 = (-\tilde{H}_y, \tilde{H}_x)$. The decomposed TM-mode and TE-mode wavefields are connected to the measurements through composition matrices $\tilde{\mathbf{L}}_{1,2}$. The decomposed down- and upgoing TM- and TE-modes are stored in the vector $\tilde{\boldsymbol{P}} = (\tilde{\boldsymbol{p}}^+, \tilde{\boldsymbol{p}}^-)$, and $\tilde{\boldsymbol{p}}^\pm = (\tilde{p}^\pm_{TM}, \tilde{p}^\pm_{TE})$, where $^+$ denotes a downgoing wave and $^-$ an upgoing wave. The fields are composed of the down- and upgoing wavefields as $\tilde{\boldsymbol{F}}_1 = \tilde{\mathbf{L}}_1(\tilde{\boldsymbol{p}}^+ + \tilde{\boldsymbol{p}}^-)$ and $\tilde{\boldsymbol{F}}_2 = \tilde{\mathbf{L}}_2(\tilde{\boldsymbol{p}}^+ - \tilde{\boldsymbol{p}}^-)$. The down- and upgoing modes are obtained form the measured data by $\tilde{\boldsymbol{p}}^\pm = -(\tilde{\mathbf{L}}_2^t\tilde{\boldsymbol{F}}_1 \pm \tilde{\mathbf{L}}_1^t\tilde{\boldsymbol{F}}_2)$ where the superscript ^{t} denotes matrix transposition. Expressions for the composition matrices can be found in [5]. This choice of $\tilde{\mathbf{L}}_{1,2}$ is known as flux-normalization and has the advantage that upgoing and downgoing transmission responses are equal [9]. The two modes are independent from each other and, e.g., the TE-mode impulse reflection response of the layered medium at the receiver level is given by $\tilde{R}_0^{TE} = \tilde{p}^-_{TE}/\tilde{p}^+_{TE}$ and can be written as

$$\tilde{R}_0^{TE} = \frac{\Gamma(\mathrm{i}k_y\tilde{E}_x - \mathrm{i}k_x\tilde{E}_y) - \zeta(\mathrm{i}k_x\tilde{H}_x + \mathrm{i}k_y\tilde{H}_y)}{\Gamma(\mathrm{i}k_y\tilde{E}_x - \mathrm{i}k_x\tilde{E}_y) + \zeta(\mathrm{i}k_x\tilde{H}_x + \mathrm{i}k_y\tilde{H}_y)}, \quad (1)$$

where the vertical wavenumber is denoted Γ and is given by $\Gamma = \sqrt{\kappa^2 + \eta\zeta}$ and $\kappa^2 = k_x^2 + k_y^2$ is the radial wavenumber, and $\eta = \mathrm{i}\omega\varepsilon$, $\zeta = \mathrm{i}\omega\mu$. The electric permittivity is denoted ε and magnetic permeability is indicated by μ, which together determine the propagation velocity $c = 1/\sqrt{\varepsilon\mu}$.

Two important observations can be made. The impulse reflection response of either mode only depends on the radial wavenumber κ and when we scale the radial wavenumber as $\kappa = \omega p$, with p being radial slowness, the local reflection coefficients are independent of frequency under our assumption of a lossless layered medium. The TE-mode local reflection coefficient of a reflector at depth level z_n is given by

$$r_n^{TE} = \frac{\mu_{n+1}\sqrt{1/c_n^2 - p^2} - \mu_n\sqrt{1/c_{n+1}^2 - p^2}}{\mu_{n+1}\sqrt{1/c_n^2 - p^2} + \mu_n\sqrt{1/c_{n+1}^2 - p^2}}. \quad (2)$$

Now that we have the impulse reflection response from the measured data we investigate how this can be used to focus the wavefield in a point in the subsurface. This can be done for each mode separately and we treat the general case.

III. Directional Green's function representations for a buried virtual receiver

In this section we give two Green's function representations for a buried virtual receiver in terms of down- and upgoing parts, $\tilde{f}^\pm$, of a focusing wavefield $\tilde{f}$ and the impulse reflection response R_0, where from here onward we omit the explicit indication of the mode. Green's function representations are obtained using the reciprocity theorems of the time-convolution and time-correlation types [10]. Here we just give the results similar as those obtained in [11], where the virtual receiver is located at the focusing depth level z_i $z_i > z^r$,

$$\tilde{G}^-(p, z_i, z^r, \omega) + \tilde{f}^-(p, z^r, z_i, \omega) = \tilde{f}^+(p, z^r, z_i, \omega)\tilde{R}_0(p, z^r, \omega), \quad (3)$$

$$-\tilde{G}^+(p, z_i, z^r, \omega) + [\tilde{f}^+(p, z^r, z_i, \omega)^* = [\tilde{f}^-(p, z^r, z_i, \omega)]^*\tilde{R}_0(p, z^r, \omega), \quad (4)$$

where * denotes complex conjugation. These two relations can be understood as follows. The functions $\tilde{f}^\pm$ are the up- and downgoing parts of a focusing wavefield that obeys the homogeneous wave equation in a medium that is the same as the actual layered medium between the receiver level z^r and the focusing depth level z_i and homogeneous below z_i. The focusing wavefield focuses at depth level z_i, hence $\tilde{f}^+(p, z_i, z_i, \omega) = 1$ and $\tilde{f}^-(p, z_i, z_i, \omega) = 0$. At the receiver level they are related to each other through the impulse reflection response of the medium that is layered up to z_i, as depicted in Figure 1. The up- and downgoing Green's functions are the VRP Green's functions for an upgoing and downgoing field at the depth level z_i and generated by a downgoing source wavefield at the receiver level z^r, see Figure 2. Notice that for the Green's function z_i is the receiver depth level and z^r is the source depth level. Now we can interpret equations (3) and (4). Equation (3) says that if we convolve in the time domain the downgoing part of the focusing wavefield with the layered earth reflection response, we obtain the upgoing part of focusing wavefield and the Green's function that corresponds to the upgoing wavefield measured at z_i that is generated by a source wavefield at z^r. Equation (4) says that if we correlate in the time domain the upgoing part of the focusing wavefield with the layered earth reflection response, we obtain the time-reverse of the downgoing part of focusing wavefield minus the Green's function that corresponds to the downgoing wavefield measured at z_i that is generated by a source wavefield at z^r.

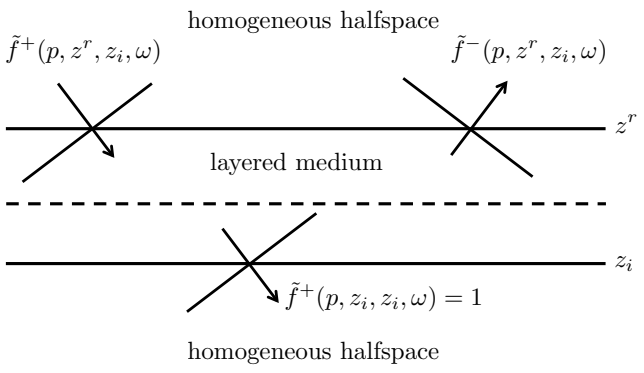

Fig. 1. The focusing wavefield $\tilde{f}^\pm$ at the surface z^r and focus level z_i.

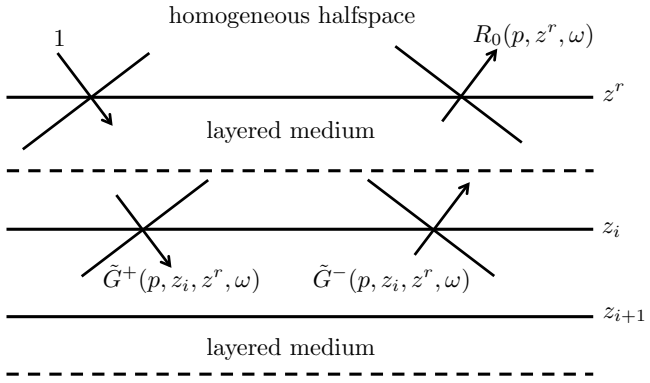

Fig. 2. The unit function as incident wavefield and the impulse reflection response at the surface z^r and the corresponding up- and downgoing Green's functions at the focusing depth level z_i.

IV. The character of the focusing wavefield

Let us take a closer look at the focusing wavefield first. The medium for which the focusing wavefield is defined is layered between the depth levels z^r and z_i and is homogeneous outside this region. If the downgoing wavefield just above z^r would be a downward propagating unit amplitude plane wave the upgoing wavefield would be the reflection response corresponding to that medium. This reflection response is denoted $\tilde{R}_0^i(p, z^r, \omega)$, where the superscript ^{i} is introduced to denote that the reflection response belongs to the medium that is homogeneous below z_i. The downgoing wavefield below the depth level z_i would be the transmission response of that medium, which we could write it as $T_0^i(p, z_i, z^r, \omega)$. Because the focusing wavefield is defined as the wavefield that has unit amplitude at depth level z_i, we find $\tilde{f}^+(p, z^r, z_i, \omega) = [\tilde{T}_0^i(p, z_i, z^r, \omega)]^{-1}$ and $\tilde{f}^-(p, z^r, z_i, \omega) = \tilde{R}_0^i(p, z^r, \omega)/\tilde{T}_0^i(p, z_i, z^r, \omega)$. Hence, $\tilde{f}^+(p, z_i, z_i, \omega) = 1$ and we have obtained our desired focusing wavefield. For simplicity we take the simplest example possible, that of a medium with two reflectors, at z_0 and z_1 and the source and receiver just above z_0. If we emit a single pulse at $t = 0$ at $z = z_0$ the downgoing and upgoing wavefields just above z_0 and just below z_1 are given by

$$\tilde{p}^+(z_0, t) = \delta(t), \tag{5}$$

$$\tilde{p}^-(z_0, t) = r_0\delta(t) + \tau_0^2 r_1 \sum_{m=0}^{\infty} (-r_0 r_1)^m \delta(t - 2(m+1)t_1), \tag{6}$$

$$\tilde{p}^+(z_1, t) = \tau_0\tau_1 \sum_{m=0}^{\infty} (-r_0 r_1)^m \delta(t - (2m+1)t_1), \tag{7}$$

where the explicit dependence on the radial slowness is omitted for brevity. The local reflection coefficient of the reflector at z_i is denoted r_i and the local transmission coefficient is denoted τ_i. The travel time from depth level z_0 to z_1 is given by $t_1 = (z_1 - z_0)\sqrt{1 - c_1^2 p^2}/c_1$. The downgoing part of the focusing wavefield is the inverse of the downgoing impulse transmission response and we can find this as

$$\tilde{f}^+(p, z_0, z_1, t) = \frac{\delta(t + t_1) + r_0 r_1 \delta(t - t_1)}{\tau_0\tau_1}. \tag{8}$$

We can find $\tilde{f}^+(z_1, z_1, t)$ by convolving $\tilde{f}^+(p, z_0, z_1, t)$ with $\tilde{p}^+(p, z_1, t)$ to find $\tilde{f}^+(p, z_1, z_1, t) = \delta(t)$. We can also find $\tilde{f}^-(p, z_0, z_1, t)$ by convolving $\tilde{f}^+(p, z_0, z_1, t)$ with $\tilde{p}^-(p, z_0, t)$ to find

$$\tilde{f}^-(p, z_0, z_1, t) = \frac{r_0\delta(t + t_1) + r_1\delta(t - t_1)}{\tau_0\tau_1}. \tag{9}$$

We observe that at the receiver level z_0 both up- and downgoing parts of the focusing wavefield have two terms that arrive within the time window $|t| \leq t_1$. Apart from the scaling factor $(\tau_0\tau_1)^{-1}$ the upgoing part contains the correct local reflection coefficient r_1 at $t = t_1$. This result can be generalized to any number of layers as was already shown before [12]. The downgoing part of the focusing wavefield is the inverse of the impulse transmission response and for a layered medium with reflectors from z_0 to z_i it will have 2^i number of events in the time window $-t_d(p, z_i, z_0) \leq t \leq t_d(p, z_i, z_0)$, where t_d denotes the direct arrival from the source at z_0 to the receiver at z_i. The upgoing part of the focusing wavefield has the same number of events in the same time window.

V. Obtaining the focusing wavefield from the impulse reflection response

In the time-domain the upgoing and downgoing parts of the Green's function in the time-domain equivalents of equations (3) and (4) are causal functions of time and therefore they are zero before the direct arrival from the level z^r to the level z_i. Let us assume for simplicity that the receiver level is just above z_0 then $\tilde{G}^{\pm}(p, z_i, z_0, t) = 0$ for $t \leq t_d(p, z_i, z_0)$. Hence for $t < t_d(p, z_i, z_0)$ in the time-domain equivalents of equations (3) and (4) can be written without the Green's functions, because they are still zero. The time-instant $t = \pm t_d$ is part of the equations, but the equations are not valid without the Green's functions for this time-instant. Therefore, $\tilde{f}^+(p, z_0, z_i, -t_d)$ is needed and we must find an estimate of the first event of the focusing wavefield, $\tilde{f}^+(p, z_0, z_i, -t_d)$. We have seen in the example of the focusing wavefield that the first event at the receiver level z_0 is a time-advanced impulse scaled by the product of local transmission coefficients. We have also seen that not using this scaling factor will result in the correct local reflection amplitude at the arrival time corresponding to that reflector. We can therefore ignore the scaling factor and emit a unit amplitude impulse, but still we need to find the one-way travel time t_d from the source level to the receiver level. In the slowness-time domain, the recording time is the apparent travel-time or intercept time. This is twice the vertical travel time from the source level to the reflector level. Hence, for every recording time instant, the focus time t_d is half the recording time. We will create focus times and retrieve the local reflection coefficients from the upgoing focusing wavefield at $t = t_d$. We split the downgoing

focusing wavefield up in a direct part and a coda as

$$\tilde{f}^{+}(p,z_0,z_i,t)=\frac{\delta(t+t_d)+M^{+}(p,z_0,z_i,t)}{\tau_0\tau_1\tau_2\cdots\tau_i}, \tag{10}$$

where the coda is denoted $M^{+}(p,z_0,z_i,t)$ and also scaled by the product of local transmission coefficients, and $M^{+}(p,z_0,z_i,t)=0$ for $t\leq -t_d$. Since $\tilde{f}^{-}(p,z_0,z_i,t)$ is the reflection response to $\tilde{f}^{+}(p,z_0,z_i,t)$ we can take $\tilde{f}^{-}(p,z_0,z_i,t)=0$ for $t=t_d$. We use the same scaling factor in the upgoing focusing wavefield as

$$\tilde{f}^{-}(p,z_0,z_i,t)=\frac{M^{-}(p,z_0,z_i,t)}{\tau_0\tau_1\tau_2\cdots\tau_i}. \tag{11}$$

Substitutions of these choices in the time-domain equivalents of equations (3) and (4) yields the final equations

$$M^{-}(p,z_0,z_i,t)=\tilde{R}_0(p,z_0,t+t_d) + \int_{-t_d}^{t} M^{+}(p,z_0,z_i,t')\tilde{R}_0(p,z_0,t-t')\mathrm{d}t', \tag{12}$$

$$M^{+}(p,z_0,z_i,t)=\int_{-t}^{t_d} M^{-}(p,z_0,z_i,t')\tilde{R}_0(p,z_0,t'-t)\mathrm{d}t', \tag{13}$$

valid for $-t_d<t<t_d$ and that can be solved numerically for $M^{\pm}$. Equations (12) and (13) are related to the Marchenko equation in [6] for which reason we call these equations coupled Marchenko-type equations.

VI. Obtaining estimates of the medium parameters

Once equations (12) and (13) are solved for one particular focus time t_d and one particular radial slowness value p the local reflection coefficient corresponding to that time is retrieved from the upgoing part of the focusing wavefield

$$r_i(p)=\int_{t_d-\epsilon}^{t_d} M^{-}(p,z_0,z_i,t)\mathrm{d}t, \tag{14}$$

where ϵ is an infinitesimal number. This is then done for all values of p available in the data and for all focus times.

To arrive at this result we had to extract the reflection response from the measured electric and magnetic fields. This was done by decomposing the measured electric and magnetic fields into up- and downgoing TE- and TM-modes, and obtaining the reflection responses, as shown in equation (1) for the TE-mode. To do that we needed the medium parameters of the layer in which the actual receivers are located. After that step no other model information was used. Imaging in this way is a data-driven imaging method, because we first retrieve the focusing wavefield from the measured reflection response and then extract the image from the upgoing part of the focusing wavefield. We call this Marchenko imaging.

We now continue to use the image to extract the medium parameters and finally to convert image times to image depths. The local reflection coefficient for depth level z_i in the TE-mode is given by equation (2). From the image containing all local reflection coefficients at apparent one-way vertical travel time we can start at the first reflector and obtain a least-squares solution for the electric permittivity and magnetic permeability below the reflector from the general expression, which can be made explicit for discrete values of p as $p_n=n\Delta p$, $n=0,1,2,\cdots,N$, in a matrix equation for ε_{i+1} and μ_{i+1} as

$$\mathbf{A}\boldsymbol{u}=\boldsymbol{b}, \tag{15}$$

with

$$\mathbf{A}=\begin{pmatrix} 1 & 0 \\ 1 & (p_1c_0)^2 \\ 1 & (p_2c_0)^2 \\ \vdots & \vdots \\ 1 & (p_Nc_0)^2 \end{pmatrix}, \boldsymbol{u}=\begin{pmatrix} \frac{\varepsilon_{r;i+1}}{\mu_{r;i+1}} \\ \mu_{r;i+1}^{-2} \end{pmatrix} \tag{16}$$

where $\varepsilon_{r;i+1},\mu_{r;i+1}$ are the relative medium parameters of layer $i+1$, e.g., $\varepsilon_{i+1}=\varepsilon_0\varepsilon_{r;i+1}$ and a similar definition is used for μ. Each element b_m, $m=0,1,2,\cdots,N$, of the vector $\boldsymbol{b}$ is given by

$$b_m=\left(\frac{1-r_i^{TE}(p_m)}{1+r_i^{TE}(p_m)}\right)^2\frac{\varepsilon_{r;i}\mu_{r;i}-(p_mc_0)^2}{\mu_{r;i}^2}. \tag{17}$$

The least squares solution is obtained as $\boldsymbol{u}=\mathbf{K}\boldsymbol{q}$ with $\mathbf{K}=(\mathbf{A}^t\mathbf{A})^{-1}$ and $\boldsymbol{q}=\mathbf{A}^t\boldsymbol{b}$. This is a simple 2×2 matrix problem for which the solution can be written down directly

$$\mu_{r;i+1}=1/\sqrt{K(2,1)q(1)+K(2,2)q(2)}, \tag{18}$$

$$\varepsilon_{r;i+1}=\mu_{r;i+1}(K(1,1)q(1)+K(1,2)q(2)). \tag{19}$$

We start in the air with $i=0$ where the receivers are present and work our way down into the layered medium. Starting by assuming we know the medium parameters in air, $\varepsilon_{r;0}=1$, and $\mu_{r;0}=1$, we find the least squares solution recursively for the layer below an interface. Once we have the electric and magnetic parameters, we know the propagation velocities inside each layer and can transform the one-way vertical travel time for $p=0$ to depth. With this last step the full waveform inversion is complete.

VII. Numerical results

We give an example of the scheme and use a nine-layer model, with eight reflecting interfaces, and properties given in Table I. The first height is the source and receiver height above the first reflector. For the data modeling we use a 250 MHz center frequency Ricker wavelet. We use offsets such that plane waves traveling at 35 degrees from the vertical axis can

TABLE I
MODEL PARAMETERS FOR THE FORWARD MODEL.

layer #	ε_r (-)	μ_r(-)	h (m)
1	1.00	1.00	1.75
2	3.90	1.00	1.57
3	2.40	1.00	0.71
4	4.20	1.00	1.70
5	9.10	1.40	1.21
6	16.1	1.50	1.10
7	12.3	1.39	1.23
8	9.10	1.25	1.51
9	13.3	1.31	∞

be retrieved in the plane wave reflection response after decomposition and transforming the data to the tau-p domain. The angles of incidence used in the figures are related to the angles in the air and hence angle, α, and ray-parameter p are related through $p = \sin(\alpha)/c_0$. The modeled data is used to find the up- and downgoing focusing wavefields $M^{\pm}(p, z_0, z_i, t)$ from equations (12) and (13). From $M^{-}(p, z_0, z_i, t)$ we find the local reflection coefficient using equation (14). Notice that we find the image as a time image because the one-way vertical arrival time for each plane wave is half the intercept time in the data. This result is shown in Figure 3 where the retrieved image is shown in red dashed-dotted lines overlaying the black solid lines that correspond to the model values computed using the medium parameters given in Table I. No visible differences occur in the image result, demonstrating that the Marchenko imaging procedure accurately retrieves the correct amplitudes at the correct image times.

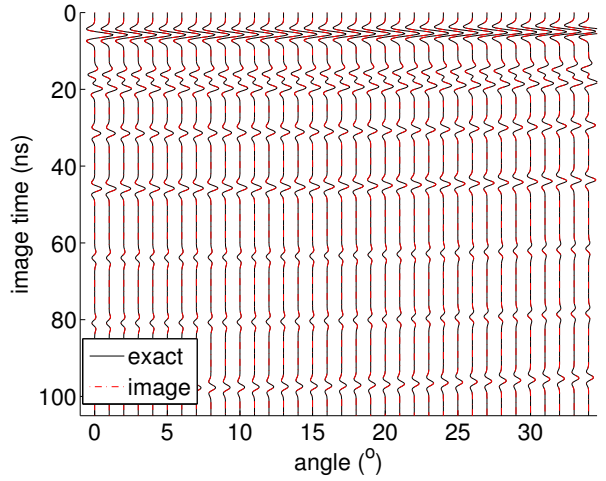

Fig. 3. The image as a function of incidence angle and one-way intercept, or image, time, black solid lines indicate the exact result and the red dashed-dotted lines indicate the numerical result.

We identify the eight reflectors in the image and pick the image times that correspond to the extrema as a function of angle of incidence for each reflection event. We then use the inversion method described by equations (18) and (19) to compute ε_r and μ_r from the reflection coefficient values. It is a recursive scheme, so we start at the first reflector and work our way down into the layered medium. The results of the medium parameters and associated errors are shown in Table II where the inversion results are shown. The errors shown in the table are computed according to following general formula $\text{err} = 100(|f^{mod} - f^{inv}|)/f^{mod}$, where f can be ε_r, μ_r, or h, and err is given in %. From the table it can be seen that the largest errors occur in the medium parameters of layer 6 where ε is underestimated by 3.3% and μ by 4.2%. Once the electromagnetic parameters are obtained in each layer, the image times can be converted to image depths and the results are also give in Table II together with the errors. Again the largest error occurs in the thickness estimate of layer six and its thickness is overestimated by 3.9%.

TABLE II
VALUES FOR INVERTED MODEL PARAMETERS AND THEIR ERRORS.

layer #	ε_r (-)	err (%)	μ_r(-)	err (%)	h (m)	err (%)
1	1.00	0.0	1.00	0.0	1.75	0.0
2	3.89	0.2	1.00	0.3	1.57	0.2
3	2.37	1.3	1.00	1.1	0.72	1.2
4	4.19	0.2	1.00	0.5	1.71	0.4
5	8.99	1.3	1.38	1.8	1.23	1.5
6	15.6	3.3	1.44	4.2	1.14	3.9
7	12.0	2.1	1.35	2.8	1.26	2.5
8	8.99	1.2	1.23	1.6	1.53	1.4
9	13.0	2.1	1.27	3.2	–	–

VIII. Conclusion

From the results we can conclude that the coupled Marchenko equations lead to accurate image times and amplitudes that can be further used in an inversion step. The accuracy of both image times and amplitudes lead to very accurate estimates of the electric permittivity and magnetic permeability. These estimates are used to convert image times to accurate layer thickness estimates. The largest error in the estimates was around 4%. Of course these results are obtained using noise free data, but the example shows that in principle the method works well for finite frequency bandwidth data. How the method will perform on noisy data remains to be investigated.

References

[1] R. L. Weaver and O. I. Lobkis, "Ultrasonics without a source: Thermal fluctuation correlations at MHz frequencies," *Physical Review Letters*, vol. 87, no. 13, pp. 134 301–1–4, 2001.

[2] K. Wapenaar, "Retrieving the elastodynamic Green's function of an arbitrary inhomogeneous medium by cross correlation," *Phys. Rev. Lett.*, vol. 93, no. 25, pp. 254 301–1–4, 2004.

[3] E. Slob, D. Draganov, and K. Wapenaar, "Interferometric electromagnetic Green's functions representations using propagation invariants," *Geophysical Journal International*, vol. 169, no. 1, pp. 60–80, 2007.

[4] K. Wapenaar, E. Slob, and R. Snieder, "Seismic and electromagnetic controlled-source interferometry in dissipative media," *Geophysical Prospecting*, vol. 56, no. 3, pp. 419–434, 2008.

[5] E. Slob, "Interferometry by deconvolution of multi-component multi-offset GPR data," *IEEE Trans. Geoscience and Remote Sensing*, vol. 47, no. 3, pp. 828–838, March 2009.

[6] K. Wapenaar, F. Broggini, E. Slob, and R. Snieder, "Three-dimensional single-sided marchenko inverse scattering, data-driven focusing, green's function retrieval, and their mutual relations," *Physical Review Letters*, vol. 110, p. 084301, Feb 2013. [Online]. Available: http://link.aps.org/doi/10.1103/PhysRevLett.110.084301

[7] J. H. Rose, "Single-sided autofocusing of sound in layered materials," *Inverse Problems*, vol. 18, pp. 1923–1934, Dec 2002.

[8] J. Kong, "Electromagnetic fields due to dipole antennas over stratified anisotropic media," *Geophysics*, vol. 37, no. 6, pp. 985–996, 1972.

[9] B. Ursin, "Review of eleastic and electromagnetic wave propagation in horizontally layered media," *Geophysics*, vol. 48, pp. 1063–1081, 1983.

[10] C. P. A. Wapenaar and J. L. T. Grimbergen, "Reciprocity theorems for one-way wavefields," *Geophysical Journal International*, vol. 127, no. 1, pp. 169–177, OCT 1996.

[11] E. Slob and K. Wapenaar, "Gpr wave field decomposition, synthesis and imaging for lossless layered vertically transverse isotropic media," in *Proceedings of the 7th International Workshop on Advanced GPR*. IEEE, 2013, pp. 1–6.

[12] P. L. Goupillaud, "An approach to inverse filtering of near surface effects from seismic records," *Geophysics*, vol. 26, no. 6, pp. 754–760, 1961.